Title: Cleavage and perception by an inactive RLK regulate cell death mediated by *Arabidopsis* GRIM REAPER

Running title: Proteolytic GRI cleavage and receptor-interaction

Authors:

Michael Wrzaczek[1*‡], Julia P Vainonen[1*], Simon Stael[2,3,6,7], Liana Tsiatsiani[2,3,6,7,10], Hanna Help-Rinta-Rahko[1,4], Adrien Gauthier[1], David Kaufholdt[1,11], Benjamin Bollhöner[5], Airi Lamminmäki[1], An Staes[6,7], Kris Gevaert[6,7], Hannele Tuominen[5], Frank Van Breusegem[2,3], Ykä Helariutta[1,4,8], Jaakko Kangasjärvi[1,9‡]

Addresses
[1]Plant Biology, Department of Biosciences, University of Helsinki, FI-00014 Helsinki, Finland.
[2]Department of Plant Systems Biology, VIB, 9052 Ghent, Belgium
[3]Department of Plant Biotechnology and Bioinformatics, Ghent University, 9052 Ghent, Belgium
[4]Institute of Biotechnology, University of Helsinki, FI-00014 Helsinki, Finland.
[5]Umeå Plant Science Centre, Department of Plant Physiology, Umeå University, SE-90187 Umeå, Sweden.
[6]Department of Medical Protein Research, VIB, 9000 Ghent, Belgium
[7]Department of Biochemistry, Ghent University, 9000 Ghent, Belgium
[8]The Sainsbury Laboratory, University of Cambridge, Cambridge CB2 1LR, UK.
[9]Distinguished Scientist Fellowship Program, College of Science, King Saud University, Riyadh 11451 Saudi Arabia.
[10]Current address: Biomolecular Mass Spectrometry and Proteomics, Utrecht Institute for Pharmaceutical Sciences and Bijvoet Centre for Biomolecular Research, Utrecht University, NL-3584 CH Utrecht, The Netherlands.
[11]Current address: Institute of Plant Biology, Braunschweig University of Technology, DE-38106 Braunschweig, Germany.

* MW and JPV contributed equally to this work.

‡ **Corresponding authors:**

Michael Wrzaczek
Plant Biology
Department of Biosciences
University of Helsinki
POB 65 (Viikinkaari 1)
FI-00014 Helsinki
Finland
Tel: +358 2941 57773
Fax: +358 2941 59552
Email: michael.wrzaczek@helsinki.fi

Prof. Jaakko Kangasjärvi
Plant Biology
Department of Biosciences
University of Helsinki
POB 65 (Viikinkaari 1)
FI-00014 Helsinki
Finland
Tel: +358 2941 59444
Fax: +358 2941 59552
Email: jaakko.kangasjarvi@helsinki.fi

Abstract

Perception of extracellular peptides by plasma membrane-localized receptor proteins is commonly used in signal transduction. In plants especially, very little is known about how extracellular peptides are processed and activated in order to allow recognition by receptors. Here we show that induction of cell death *in planta* by a secreted plant protein GRIM REAPER (GRI) is dependent on the activity of a type II metacaspase METACASPASE-9. GRI is cleaved by METACASPASE-9 *in vitro* resulting in the release of an 11 amino acid peptide. This 11 amino acid subfragment of GRI bound *in vivo* to the extracellular domain of the plasma membrane-localized, atypical leucine-rich repeat receptor-like kinase POLLEN-SPECIFIC RECEPTOR-LIKE KINASE 5 (PRK5), and was sufficient to induce oxidative stress/ROS-dependent cell death. This shows a signaling chain in plants from processing and activation of an extracellular protein to perception by its receptor.

Keywords

Ligand / Protease / Receptor-like kinase / Secreted protein

Introduction

Perception of extracellular signals is central for plant development and survival. Plant encoded extracellular peptides and proteins are important components for developmental (e.g. meristem cell proliferation, stomatal patterning, and control of self-incompatibility) and stress response regulators (e.g. damage-associated molecular patterns; DAMPs; Boller and Felix, 2009;Butenko *et al.*, 2009). In the immune response, plants also recognize pathogen-associated molecular patterns (PAMPs) of microbial origin (Boller and Felix, 2009). The *Arabidopsis thaliana* genome encodes several hundred secreted proteins (Butenko *et al.*, 2009;Murphy *et al.*, 2012)and more than 400 membrane-spanning receptor-like protein kinases (RLKs) (Shiu and Bleecker, 2003). This suggests a large number of potential ligand-receptor interactions providing a complex network of extracellular signaling modules in plants (Boller and Felix, 2009). Nonetheless, only a few peptide-receptor interactions have so far been identified (Butenko *et al.*, 2009). In known plant extracellular ligand-receptor systems the peptide ligands are either small (e.g. Systemin, PEP1, CLAVATA) or only a short stretch of amino acids (aa) within the proteins (e.g. flg22, elf18) is recognized by their receptor (Altenbach and Robatzek, 2007; Boller and Felix, 2009). In animals, a number of secreted proteins are processed by proteolytic cleavage to release the active signaling peptide (Pimenta and Lebrun, 2007) and in plants similar mechanisms are involved in peptide activation (Murphy *et al.*, 2012).

The almost 700 proteases (Rawlings *et al.*, 2014;Tsiatsiani *et al.*, 2012) encoded in the *Arabidopsis* genome have diverse functions and specificities ranging from the processing of signal peptides required for subcellular targeting to degradation of proteins (van der Hoorn, 2008). However, plant protease substrates remain largely unexplored (Tsiatsiani *et al.*, 2012). Metacaspases, distant relatives of animal caspases (Tsiatsiani *et al.*, 2011;Vercammen *et al.*, 2007), are a class of cysteine-dependent proteases in plants, fungi and protozoa. Metacaspases are important regulators of biotic and abiotic stress responses, development and cell death in plants (Coll *et al.*, 2010;He *et al.*, 2008;Hoeberichts *et al.*, 2003;Tsiatsiani *et al.*, 2011;Vercammen *et al.*, 2007;Watanabe and Lam, 2011). To date several substrates have been identified for plant metacaspases (Tsiatsiani *et al.*, 2011) - a Tudor staphylococcal nuclease (Sundström *et al.*, 2009) in *Picea abies* and a number of substrates for *Arabidopsis thaliana* METACASPASE-9 (AtMC9; Tsiatsiani *et al.*, 2013;Vercammen *et al.*, 2006). However, there

are no instances reported for plants where a protease processes a secreted (pre)protein thereby producing a ligand for a known receptor in a specific biological process.

We have previously described an ozone (O_3) sensitive *Arabidopsis* mutant named *grim reaper* (*gri*; Wrzaczek *et al.*, 2009b). The cause for the O_3 sensitivity of the mutant was the presence of a truncated fragment of GRI in the *gri* insertion mutant. A 66-aa fragment of the secreted GRI protein, that is present in the mutant, induced cell death, as measured by elevated ion leakage, upon infiltration into plant leaves. Cell death induction by GRI-peptide was dependent on the plant hormone salicylic acid but also on production of extracellular superoxide. The *gri* mutant displayed enhanced resistance to a virulent bacterial pathogen.

Here we show that a subfragment of *Arabidopsis* GRI contains sufficient information to induce elevated ion leakage. A metacaspase, AtMC9 (Bollhöner *et al.*, 2013), is required *in vivo* for the activation of GRI in the extracellular space and is able to directly cleave GRI *in vitro*. Perception of the peptide released by AtMC9 is dependent upon binding to POLLEN-SPECIFIC RECEPTOR-LIKE KINASE 5 (PRK5), an atypical, enzymatically inactive RLK, which serves as a receptor for the peptide. Our results are an important step in understanding the processing of extracellular peptide ligands and their perception through receptors.

Results

A 20-aa GRI peptide contains information sufficient to induce elevated ion leakage. The extracellular *Arabidopsis* protein, GRIM REAPER (GRI) is involved in reactive oxygen species (ROS)-mediated cell death (Wrzaczek *et al.*, 2009b). Under superoxide-producing conditions infiltration of a 66-aa part of GRI, $GRIp^{31-96}$ that is present in the *gri*-mutant, into *Arabidopsis* leaves induced cell death, as measured by elevated ion leakage (Fig. 1A). Background ion leakage in the control infiltration (with GST) is caused by the wounding due to mechanical stress of infiltration (Fig. 1A). When testing four shorter and overlapping peptides (Supplementary information [SI] Fig S1A) in the leaf infiltration assay, only the 20-aa peptide $GRIp^{65-84}$ induced ion leakage similarly to bacterially produced GST- $GRIp^{31-96}$ and biochemically pure $GRIp^{31-96}$ (Fig. 1A; Fig. S1B shows dead cells visualized by Trypan blue staining). The three other peptides were inactive. Notably, the 20-aa-long peptide $GRIp^{65-84}$ induced elevated ion leakage in a dose responsive manner (Fig. 1B).

A LEUCINE-RICH REPEAT RLK mediates GRI-peptide-induced ion leakage. GRI is related to the *Solanaceae* stigma-specific protein STIG1 (Goldman et al., 1994). Tomato LeSTIG1 interacted *in vitro* with the ectodomains of two RLKs, the pollen receptor kinases LePRK1 and LePRK2 (Huang *et al.*, 2014;Löcke *et al.*, 2010;Tang *et al.*, 2004). Therefore we tested the potential interaction of GRI with RLKs. Leaves from *Arabidopsis* T-DNA insertion lines for leucine-rich repeat (LRR) RLKs homologous to the two tomato RLKs were infiltrated with the 66-aa $GRIp^{31-96}$ and 20-aa $GRIp^{65-84}$ peptides and scored for cell death. Two T-DNA insertion alleles in *At1g50610* (SALK_016815 and SALK_101260) in the last exon and in the 5' UTR region, respectively, displayed reduced ion leakage levels in response to peptide infiltration (Fig. 1C). This gene has recently been named *PRK5* (Chang *et al.*, 2013). Thus, the mutants are referred to as *prk5-1* (SALK_016815; Chang *et al.*, 2013) and *prk5-2* (SALK_101260), respectively. Complementation of *prk5* with a genomic clone consisting of a 1500 base pair promoter region and the coding region of *PRK5* restored the wild type phenotype (Fig. 1D). PRK5 has previously been described as a pollen-specific RLK (Chang *et al.*, 2013), but RT-PCR analysis demonstrated the presence of low levels of *PRK5* transcript in leaves (Fig S2). While *PRK5* transcript levels are low in plant organs other than pollen tubes under normal growth conditions (Fig. S3), analysis of publically available expression data suggests that transcript

abundance is increased in response to biotic and abiotic stresses (Fig. S4-S8). Similarly *GRI* transcript abundance is lower in leaves than in flowers (Wrzaczek *et al.*, 2009b). Our previous results suggested that GRI-induced cell death as evidenced by increased ion leakage was dependent on superoxide production. Therefore we used infiltration of an enzymatic system, xanthine with xanthine oxidase (XXO), to produce superoxide in the extracellular space and analyze the response of *prk5*. Compared to wild type plants, the loss-of-function mutants *prk5* and *prk4* showed slightly less, statistically not significant (but reproducible), ion leakage as induced by extracellular superoxide while the gain-of-function mutant *gri* (Wrzaczek *et al.*, 2009b) exhibited increased sensitivity (Fig. 1E). This indicates that in leaves PRK5 could act as a downstream element for ROS-dependent cell death induced by GRI or a smaller subdomain of it.

PRK5 is a plasma membrane-localized, enzymatically atypical protein kinase. PRK5 belongs to the LRR RLK subtype III (Shiu and Bleecker, 2003) and consists of 686 aas (calculated MW: 76.86 kDa; pI 7.84). A transmembrane domain separates the extracellular region with a signal peptide from the intracellular kinase domain, which contains a Y-based sorting/endocytosis motif in the C-terminus (Fig. 2A). Structural prediction suggests that the extracellular domain (Fig. S9A) is similar to other LRR RLKs and the intracellular domain (Fig. S9B) has the overall typical sequence and structural conservation of protein kinases. The few known plant receptors for extracellular proteins are plasma membrane-localized (Aker and de Vries, 2008). We analyzed the subcellular localization of PRK5 tagged with cyan fluorescent protein (PRK5-CFP; Fig. 2B) using transient expression in *Arabidopsis* mesophyll protoplasts. PRK5-CFP co-localization with the plasma membrane marker CAAX-yellow fluorescent protein (CAAX-YFP; Kwaaitaal *et al.*, 2011) (Fig. 2C-F) was markedly distinct from the cytoplasmic YFP (Fig. S10A). PRK5-YFP also localized to the cell periphery in *Nicotiana benthamiana* epidermal cells (Fig. S10B-G). After plasmolysis Hechtian strands (Vahisalu *et al.*, 2008), which connect the plasma membrane to the cell wall, were visible verifying that PRK5-YFP was localized to the plasma membrane.

While the overall kinase domain structure is preserved in PRK5, critical aas in the kinase subdomains VIb and VII (Stone and Walker, 1995) are not conserved in PRK5 (Fig. 2G, Fig.

S11A and B). The aspartic acid (D) which is conserved in active RLKs (e.g. FLS2, EFR, BRI1, CRK7) is altered to histidine (H) in PRK5. In the inactive RLKs STRUBBELIG (SUB; Vaddepalli *et al.*, 2011) and BAK1-INTERACTING RECEPTOR-LIKE KINASE 2 (BIR2; Halter *et al.*, 2014b) this residue is changed to asparagine (N). This suggested that PRK5 could be enzymatically inactive and accordingly, recombinant GLUTATHIONE S-TRANSFERASE (GST)-tagged PRK5 (GST-PRK5) did not have kinase activity towards the artificial substrate myelin basic protein. Intriguingly, mutations restoring the consensus kinase sequence in the catalytic core (H500D A520G; Fig. S11C) turned GST-PRK5 into an active kinase in the presence of $MnCl_2$ (Fig. 2H) and $MgCl_2$ (Fig. S11D). Taken together, PRK5 closely resembles an active kinase based on sequence and modeling, but, at least *in vitro*, is enzymatically inactive.

PRK5 binds GRIp$^{31\text{-}96}$ *in vitro*. Since PRK5 was required for cell death induction by GRIp$^{31\text{-}96}$ and GRIp$^{65\text{-}84}$, we investigated the interaction between GRI and the ectodomain of PRK5 *in vitro*. Recombinant full length GRI (minus signal peptide; GRI$^{31\text{-}168}$) or GRI$^{31\text{-}96}$ fused to GST were incubated with ^{35}S-methionine-labeled *in vitro* produced extracellular domains of PRK5$^{40\text{-}281}$ or PRK4$^{40\text{-}279}$. GRI$^{31\text{-}96}$ interacted directly with PRK5$^{40\text{-}281}$, while GRI$^{31\text{-}168}$ showed slightly weaker interaction (Fig. 3A; Fig. S12 shows Western analysis with α-GST, α-GRI and α-GRI-peptide antibodies). Binding of GRI$^{31\text{-}96}$ and GRI$^{31\text{-}168}$ to the PRK4 extracellular domain was weaker compared to binding of GRI$^{31\text{-}96}$ to PRK5$^{40\text{-}281}$ (Fig. 3A). Given the high sequence similarity of PRK4 and PRK5 (70.15 % sequence identity; 77.76 % sequence similarity; Fig. S12E) it is not surprising that GRI$^{31\text{-}96}$ and GRI$^{31\text{-}168}$ were still able to interact at least to some extent with both receptors. No interaction was however detected with the ectodomain of a different RLK, FLAGELLIN-SENSITIVE 2 (FLS2; Fig. S12F). These results suggest that GRI and the 66-aa peptide GRI$^{31\text{-}96}$ can directly interact with the extracellular domains of receptors, preferentially with the ectodomain of PRK5.

Native PRK5 binds GRIp$^{65\text{-}84}$. GRIp$^{65\text{-}84}$ is a subfragment of GRIp$^{31\text{-}96}$ sufficient to induce elevated ion leakage upon infiltration into *Arabidopsis* leaves. To investigate whether the interaction of GRI and PRK5 can take place *in vivo*, an additional tyrosine (Y) was added to the N-terminus of GRIp$^{65\text{-}84}$ to allow radiolabeling with Iodine^{125} (^{125}I). The Y-GRIp$^{65\text{-}84}$ peptide showed similar activity in inducing elevated ion leakage compared to GRIp$^{65\text{-}84}$ and GRIp$^{31\text{-}96}$

(Fig. 3B). In radioligand binding assays ^{125}I-Y-GRIp$^{65-84}$ bound to membrane fractions from wild-type plants whereas binding was strongly reduced in *prk5-2* extracts, and excess of 10 µM non-radiolabeled Y-GRIp$^{65-84}$ reduced binding to background levels (Fig. 3C). ^{125}I-Y-GRIp$^{65-84}$ bound to microsomal fractions of protoplasts overexpressing PRK5-c-myc and also, albeit with lower affinity, PRK4-c-myc (Fig. 3D and E). Specific binding of ^{125}I-Y-GRIp$^{65-84}$ was competed out by non-radioactive Y-GRIp$^{65-84}$ with an IC_{50} of 25.2 nM (Fig. 3F). Of the four short peptides, only GRIp$^{65-84}$ competed for binding (Fig. 3G). Interestingly, the 66-aa-long GRIp$^{31-96}$ did not compete for binding of ^{125}I-Y-GRIp$^{65-84}$ (Fig. 3G) indicating that, even though it interacted with the ectodomain of PRK5 *in vitro*, binding activity to membrane fractions would require further processing. Reasons might be that the receptor used in the *in vitro* assay was without co-receptors or other interacting proteins which *in vivo* might set additional constraints for ligand binding. In addition, as shown in other similar systems (Löcke *et al.*, 2010), other extracellular proteins interacting with GRI might add further constraints for the ligand-receptor interaction *in vivo*. Together the results suggest that the extracellular domain of PRK5 serves as a sensor for peptides derived from GRI through direct protein-protein interaction.

A metacaspase is required for activation of GRI-peptide. Although infiltration of both the 66-aa GRIp$^{31-96}$ and the 20-aa GRIp$^{65-84}$ induced cell death *in planta* (Fig. 1A), the 66-aa peptide did not compete for binding of ^{125}I-Y-GRIp$^{65-84}$ *in vivo* (Fig. 3G). Furthermore, Western blot analysis on leaf extracts of epitope-tagged GRI overexpressing plants displayed two distinct bands (Wrzaczek *et al.*, 2009b). Together these data suggested that GRI might be processed by proteolytic cleavage (Wrzaczek *et al.*, 2009a) and analysis of GRI protein sequence suggested that the metacaspase AtMC9 might be able to cleave GRI. The *in vitro* and *in vivo* substrate specificity for AtMC9 has been described in detail (Tsiatsiani *et al.*, 2013). The sequence SKTR$^{64-67}$ in the 66-aa cell death-inducing peptide GRIp$^{31-96}$ holds the characteristic of the AtMC9 preference for basic residues at substrate positions P3 and P1 (K and R; Vercammen *et al.*, 2006;Vercammen *et al.*, 2004).

In accordance with this, recombinant AtMC9 (rAtMC9; Vercammen *et al.*, 2004) directly cleaved bacterially-produced maltose-binding protein (MBP)-GRI fusion protein *in vitro* (Fig. 4A). The inactive mutant rAtMC9^{mut} (Belenghi *et al.*, 2007) showed no proteolytic activity

towards MBP-GRI (Fig. 4A). The shift in the molecular weight of MBP-GRI$^{25-168}$ in Western blot analysis with α-MBP antibody suggested cleavage of GRI at the SKTR motif which is located at the N-terminus of GRIp$^{65-84}$. The position of the AtMC9 cleavage site(s) in the MBP-GRI$^{25-168}$ protein was determined by LC-MS/MS following in-solution labeling with a trideutero-acetyl group (<AcD3>) of primary alpha-amines of newly formed N-termini generated by AtMC9 cleavage. Analysis led to the identification of the peptides <AcD3>-^{68}LLVSHYK^{74} and <AcD3>-^{98}GTSLLHCCK^{107}, thus showing that *in vitro* AtMC9 cleaves MBP-GRI$^{25-168}$ not only after arginine 67 (R67 of the SKTR motif) but also after lysine 97 (K97, the second K of the KANK sequence; Fig. S13A, B and C). To assess the *in vivo* relevance of GRI-peptide cleavage by AtMC9 we used the *atmc9* mutant (Bollhöner *et al.*, 2013). The short 20-aa peptide GRIp$^{65-84}$ was able to induce cell death in *atmc9* (Fig. 4B) but not the longer 66-aa GRIp$^{31-96}$. In addition, *atmc9* displayed slight, statistically not significant but reproducible, reduction in the ion leakage induced by XXO compared to wild type plants (Fig. S14). This suggests that AtMC9 activity is required to modify the 66-aa GRIp$^{31-96}$ for the induction of elevated ion leakage.

To investigate the cleavage of GRI in more detail we analyzed the fragments generated by incubation of GRIp$^{31-96}$ (the 66-aa subfragment of GRI which is produced in the *gri* mutant; Wrzaczek *et al.*, 2009b) with rAtMC9. Reverse Phase-HPLC and mass spectrometric analysis revealed cleavage of the peptide after lysine 65 (K65) and arginine 67 (R67) in the SKTR motif and an additional site after lysine 78 (K78) in the KKIKK pattern (Fig. 4C; Fig. S15A, B and C). In combination with the results from cleavage of MBP-GRI this suggested that an 11-aa-long peptide, GRIp$^{68-78}$, could be produced by cleavage with AtMC9.

To address the relevance of this cleavage for GRI-peptide activity we tested an 11-aa peptide GRIp$^{68-78}$ (Fig. 4C). GRIp$^{68-78}$ induced cell death in Col-0 but not in *prk5-1* (Fig. 4B) or *prk5-2* (Fig. S16A). GRIp$^{68-78}$ but not GRIp$^{31-96}$ induced ion leakage in *atmc9-1* (Fig. 4B). As cell death induction by GRI-peptide is dependent on salicylic acid and extracellular superoxide (Wrzaczek *et al.*, 2009b) we tested induction of elevated ion leakage by GRIp$^{68-78}$ in mutants deficient in salicylic acid (*salicylic acid deficient 2* [*sid2*]) and extracellular superoxide production (*respiratory burst oxidase homolog* D [*rbohD*]). Neither GRIp$^{31-96}$ nor GRIp$^{68-78}$ induced elevated ion leakage in *sid2* and *rbohD* (Fig. S16B). These results suggest that salicylic acid and

extracellular superoxide are still required for cell death induction by the processed GRIp$^{68-78}$. A tyrosine-labeled version of the 11-aa peptide, Y-GRIp$^{68-78}$, also induced elevated ion leakage (Fig. 4D) and ^{125}I-labeled Y-GRIp$^{68-78}$ bound to membrane extracts from wild type plants (Fig. 4E). However, binding was reduced to background levels in *prk5-1* and *prk5-2* (Fig. 4E). Binding of ^{125}I-Y-GRIp$^{68-78}$ was competed out by addition of non-radioactive GRIp$^{68-78}$ and GRIp$^{65-84}$ but not by other peptides (Fig. 4F). The high binding background could result from anionic interactions be due to the strong basic nature of the 11-aa peptide (Fig. 4G, Fig. S17), which may affect calculation of the dissociation constant (Kd) of 1.9 nM for GRIp$^{68-78}$. The results suggest that an 11-aa peptide derived from GRI based on identified AtMC9-cleavage sites is sufficient to induce cell death in *Arabidopsis* leaves and binds with high specificity to the extracellular domain of the receptor PRK5. The *gri* mutant has previously been found to be more resistant to the virulent bacterial pathogen *Pseudomonas syringae* pv. *tomato* DC3000 (Wrzaczek *et al.*, 2009b). However, *prk5* and *atmc9* did not display altered pathogen resistance (Fig. S18). A reason for this might be that the infiltration with the pathogen into *gri* – where a "pre-activated" GRI-derived peptide could already be present - leads to a number of cells undergoing cell death which would lead to the initiation of a hypersensitive response (HR). In the *prk5* and *atmc9* mutants this pre-activated GRI-derived peptide is not present. Also, the preactivated peptide could not be perceived (in *prk5*) or produced (in *atmc9*). Thus, *prk5* and *atmc9* did not exhibit altered sensitivity to the virulent pathogen. However, more detailed analysis of this aspect will be required in the future using *prk5* and *atmc9* double mutants with *gri* but also overexpression of *prk5*. Also, a complete loss-of-function allele for *gri* will be crucial for further dissection of the roles of GRI and derived peptides.

Our hypothesis that GRI is an *in vivo* target of AtMC9 is supported by the fact that both proteins have been reported to be present in the extracellular space (Vercammen *et al.*, 2006;Wrzaczek *et al.*, 2009b). Additional lines of evidence suggest that proteolytic processing is required for the biological activity of GRI. The 66-aa GRIp$^{31-96}$ was unable to compete out the binding of radioactively labeled ^{125}I-Y-GRIp$^{65-84}$ in plant membrane fractions (Fig. 3G and Fig. 4F) and was unable to induce elevated ion leakage in the *atmc9* mutant. While metacaspases are involved in stress adaptation and cell death regulation in plants (Lam and Zhang, 2012;Tsiatsiani *et al.*, 2011), the role of AtMC9 in these processes has previously been unknown. Our results show that

AtMC9 directly cleaves GRI and is thus involved in the processing and activation of the extracellular peptide.

Discussion

In this study we describe how the secreted protein GRI is cleaved by a protease and a resulting peptide is subsequently perceived by a transmembrane receptor. GRI is a secreted *Arabidopsis* protein with similarity to Stig1 from tobacco and tomato. A 66-aa N-terminal fragment of GRI, which is produced in the gain-of-function mutant *gri*, was previously shown to induce cell death when infiltrated into *Arabidopsis* leaves (Wrzaczek *et al.*, 2009b). We show that recombinant GRI and $GRIp^{31-96}$ were cleaved by the metacaspase AtMC9 *in vitro*, releasing an 11-aa peptide (Fig. 4) that was sufficient for the induction of cell death as inferred from ion leakage measurements. Physiological evidence indicated that this metacaspase-dependent processing of GRI was required for cell death induction *in planta*.

We identified PRK5, a receptor-like kinase, as the receptor for GRI-derived peptides as generated through cleavage by AtMC9. PRK5 is required for cell death induction by GRI. PRK5 is present in leaves at low levels similarly to GRI itself. Whilst Stig1 and PRK5 have been described to function in floral organs (Chang *et al.*, 2013;Goldman *et al.*, 1994) our results show that GRI and its receptor also have functions in leaves. Involvement of a signaling component in several different processes is common for plant signaling. For example BRI1-ASSOCIATED KINASE (BAK1) has originally been described to function in brassinosteroid signaling but also has important roles in PAMP and DAMP signaling (Liebrand *et al.*, 2014).

Our *in silico* and *in vitro* analyses suggest that PRK5 is enzymatically inactive (Fig. 2G and H). Estimates indicate that 10 to 20% of all RLKs in *Arabidopsis* might be catalytically inactive (Blaum *et al.*, 2014;Castells and Casacuberta, 2007). Only a few– to our knowledge – have been linked to a biological process based on mutant analysis; examples include BIR2 (Halter *et al.*, 2014b), SUB (Vaddepalli *et al.*, 2011), and SHORT SUSPENSOR (SSR; Bayer *et al.*, 2009). While SUB has been suggested to bind a ligand (Vaddepalli *et al.*, 2011), no ligands have so far been identified for SSR. BIR2 is suggested to control BAK1-receptor complex assembly in the absence of peptide ligands and thus might not sense a ligand either (Halter *et al.*, 2014a;Halter *et al.*, 2014b). PRK5 is the first atypical, kinase-inactive, plant RLK that acts as a primary receptor for a peptide ligand.

We have previously shown that cell death induction by a 66-aa GRI peptide occurs under conditions that lead to superoxide production (Wrzaczek *et al.*, 2009b), for example through mechanical stress and wounding caused by infiltration of the peptide into *Arabidopsis* leaves. Removal of superoxide production, either by co-infiltration of the peptide with superoxide dismutase or by peptide infiltration into a mutant deficient in the NADPH oxidase RBOHD reduced cell death to background levels. Extracellular superoxide was still required for cell death induction by $GRIp^{68-78}$ (Fig. S16B). Wounding induces ROS production and is one of the signals that have been shown to initiate the so-called "ROS wave" (Mittler *et al*., 2011). Our results suggest that ROS can act as a parallel signal, perhaps together with other wound-induced cues, to sensitize cells to cell death induction by GRI-derived peptides (Fig. S19).

It is currently unknown how extracellular ROS are sensed by cells. Accurate ROS sensing most likely relies on a broad range of independent mechanisms (Wrzaczek *et al.*, 2013), and it is unlikely that ROS participate in classical ligand-receptor interactions. ROS might rather react with extracellular components including cell walls, lipids and also proteins/peptides. Whilst ROS may act as a cue in parallel to $GRIp^{68-78}$, the full-length GRI itself could be subject to redox regulation (Fig. S19) through two cysteine motifs (C-9X-C-2X-C) in its C-terminal region. The cysteine motifs in GRI are similar to the pattern found in DUF26 (domain of unknown function 26) proteins, C-8X-C-2X-C (Wrzaczek *et al.*, 2010). In both cases the cysteine motifs are suggested to be a target for redox regulation. The C-2X-C part of DUF26 and GRI also is a classical target for thioredoxins (Zhang *et al.*, 2011). Recently an extracellular thioredoxin has been shown to regulate stress responses through ROS (Zhang *et al.*, 2011). Thereby GRI could be involved in the apoplastic redox sensory mechanisms regulated through interaction with thioredoxins and reorganization of thiol bonds. This regulation could affect cleavage of GRI by modulation of the three-dimensional structure of the protein and changing accessibility of the AtMC9 cleavage sites through redox regulation of thiol bonds. Thus, GRI may be controlled dually by conformational change and proteolytic cleavage (Wrzaczek *et al.*, 2009a). GRI was not identified in a recent analysis of the AtMC9 degradome (Tsiatsiani *et al.*, 2013). However, that study was performed on young seedlings as compared to the older plants used in the work described here. It is interesting to note that AtMC9 activity can be regulated through S-nitrosylation (Belenghi *et al.*, 2007). Evidence suggests that there is significant cross-talk

between reactive nitrogen species (RNS) and ROS but the clear relationship between the two remains elusive (Wang *et al.*, 2013). The functional unit of GRI and metacaspase could be regulated by ROS/RNS on multiple levels and be part of the apoplast redox sensing machinery in plants.

GRI is a member of a small protein family with six members in *Arabidopsis*. The C-terminus of GRI containing the cysteine repeats is highly similar to Stig1 and the *Arabidopsis* orthologs but the N-terminal part after the signal peptide, which contains the cell death-inducing peptide motif, shows strikingly lower levels of conservation. Future research should address the question whether the conservation of the C-terminus of GRI is linked to cell death regulation or whether it is involved in other processes. No functions have been described for any of the GRI orthologs in *Arabidopsis*, but the conservation of the C-terminal cysteine motifs might point towards a common mode of regulation among GRI, STIG1 and related proteins. Interestingly, for CLAVATA3/ESR-RELATED 18 (CLE18) two different peptides derived from the precursor protein have been shown to have individual and possibly antagonistic functions (Murphy *et al.*, 2012). This suggests that more than one biologically active peptide could be generated from a single precursor. It remains to be determined whether this also applies to GRI and related proteins. It also remains to be seen whether GRI interacts with other extracellular proteins as has been shown for tomato LeSTIG1 (Löcke *et al.*, 2010).

The combination of GRI, AtMC9 and PRK5 provides a functional unit comprising secreted protein, protease and the receptor for the cleavage product. This scheme is likely to be employed in the regulation of many other ligand-receptor interactions in plants. Future research on the functions of GRI, AtMC9 and PRK5 in plant development including stigma-pollen interactions and cell death regulation, and the roles of the other proteins similar to GRI will increase our understanding of extracellular signaling in plants.

Materials and Methods

Plant material and growth conditions

Arabidopsis thaliana ecotype Columbia-0 (Col-0) was used as wild type. The *gri* (Wrzaczek *et al.*, 2009b) and *atmc9* (Bollhöner *et al.*, 2013) lines were previously described. The *prk5-1*, *prk5-2* and *prk4* T-DNA insertion lines were obtained from the European Arabidopsis Stock Centre (http://www.arabidopsis.info).

Seeds were sown on 1:1 peat-vermiculite mixture, stratified for 2 days and grown under controlled conditions (Vahisalu *et al.*, 2008) under 12h/12h day/night cycle (temperature 23°C/18°C, relative humidity 70%/90%). For *in vivo* radio-ligand binding assays *Arabidopsis thaliana* seedlings were grown on agar plates at 12h/12h day/night cycle, temperature 23°C/18°C for seven days.

Peptide and XXO infiltration experiments as well as pathogen infection assays were performed as previously described (Wrzaczek *et al.*, 2009b). Protoplast preparation, transfection and extracts for ligand binding assays and western analysis were prepared as described (Lee *et al.*, 2011). For transient gene expression studies, *Arabidopsis* protoplasts were transfected with PRK5-CFP, PRK4-CFP, or controls (cytoplasmic YFP, plasma membrane-localized CAAX-YFP (Kwaaitaal *et al.*, 2011) under the control of 35S promoter and incubated for 48 hours at room temperature in darkness prior to confocal microscopy.

Plasmid constructs

Constructs were created by PCR and restriction or Gateway sites were introduced *via* the PCR primers. For expression of GRI as a MBP fusion the coding sequence of GRI minus the signal peptide was cloned EcoRI/PstI into the pMAL-c2x vector (New England Biolabs). For expression of GRI as a GST fusion protein the coding sequence of GRI or $GRIp^{31-66}$ minus the signal peptide was cloned EcoRI/NotI or EcoRI/SalI, respectively, into the pGEX-4T-1 vector (GE Healthcare Life Science). The kinase domains of PRK5 and PRK4 were cloned EcoRI/NotI into pGEX-4T-1. For coupled *in vitro* transcription and translation the ectodomains of PRK5, PRK4 and FLS2 were cloned into pZeRO-2.1 (Invitrogen). For genomic complementation lines the coding region of PRK5 including 1500 bp promoter region was amplified by PCR and cloned

into pGreenII0179 (Hellens *et al.*, 2000). Plants were transformed by *Agrobacterium tumefaciens*-mediated gene transfer. Homozygous single-insert plants carrying the transgene were selected based on antibiotic resistance. The coding regions of PRK5 and PRK4 were cloned PacI/EcoRI into a modified version of the pGWR8 (Rozhon *et al.*, 2010) vector containing a 6x c-myc or YFP tag under the control of the *UBQ10* promoter. For confocal microscopy of protoplasts the coding regions of PRK5 and PRK4 were Gateway-cloned into the CZN575 vector containing the sCFP3a tag.

Trypan blue staining

Trypan blue staining was performed as described (Dat *et al.*, 2003).

GRI-derived peptides and radioiodine-labeling

Peptides were synthesized and purified to >95% purity on a reverse phase high pressure liquid chromatography by GenScript (USA), Proteogenix (France; Y-GRI$^{65-84}$ and Y-flg22) or in house on an Applied Biosystems 433A Peptide Synthesizer at VIB Ghent (GRIp$^{68-97}$). Peptides were dissolved in H_2O (stock solution 10 mg/ml), and diluted to the required concentrations just before experiments. Y-GRI$^{65-84}$ and Y-GRI$^{68-78}$ were radiolabeled with [^{125}I] iodine using chloramine-T to yield ^{125}I-Y-GRI$^{65-84}$ and Y-GRI$^{68-78}$, respectively, with a specific radioactivity >2000 Ci/mmol by BIOTREND Chemikalien (Germany).

Radio-ligand binding assays

Binding assays were performed as described (Bauer *et al.*, 2001) with modifications. Plant material (0.1g) was homogenized in 200 µl binding buffer (25 mM MES [2-(N-morpholino)ethanesulfonic acid] pH 6, 3 mM $MgCl_2$, 10 mM NaCl) containing protease inhibitor cocktail (1:100; Fermentas/Thermo Fischer Scientific). Lysates were centrifuged at 4°C for 15 minutes at 10000 x g. The pellet was resuspended in 100 µl binding buffer and filtered through Miracloth. Binding assays were incubated for 20 minutes on ice in a total volume of 100 µl with 46 fmol ^{125}I- Y-GRIp$^{65-84}$ either alone (total binding) or in presence of 10 µM Y-GRIp$^{65-84}$ or GRIp$^{65-84}$ (non-specific binding) for standard assays (concentrations for radiolabeled or cold peptides in saturation and competition assays are indicated in the figures).

Protoplasts were lysed in binding buffer containing 1% (w/v) octylphenoxypolyethoxyethanol (Nonidet NP-40), 0.1% SDS, and 0.5% (w/v) sodium deoxycholate as detergents. After 2 hours shaking at 4°C the lysates were centrifuged at 4°C for 15 minutes at 10000 x g, and the supernatant was used directly for binding assays or for immunoprecipitation with subsequent binding assays.

Membrane fractions or immunoprecipitates were collected by vacuum filtration on glass fibre filters (Macherey-Nagel MN GF-2; preincubated in binding buffer containing 1% bovine serum albumin, 1% bactopeptone, 1% bactotryptone, 1% polyethylenimine). Prior to peptide binding filters were rinsed with 1ml binding buffer. For ^{125}I- Y-GRIp$^{65-84}$ after filtration, filters were washed under constant vacuum with 1 ml binding buffer, 10 ml wash buffer I (20 mM Tris pH 7.5, 5 mM EDTA, 100 mM NaCl, 1% Triton X-100) and 5 ml wash buffer II (20 mM Tris pH 7.5, 5 mM EDTA, 1 M NaCl, 1% Triton X-100) (Jonak *et al.*, 2000). For ^{125}I-Y-GRIp$^{68-78}$ filters were washed under constant vacuum with 1 ml binding buffer and twice with 5 ml wash buffer I (20 mM Tris pH 7.5, 5 mM EDTA, 150 mM NaCl, 1% Triton X-100). Radioactivity retained on the filters was measured using a Wallac Wizard3 Gamma Counter. Specific binding was calculated by subtracting non-specific from total binding.

Western analysis of protoplasts transfected with PRK5-c-myc, PRK4-c-myc or YFP used anti-c-myc A-14 rabbit polyclonal and 9E10 mouse monoclonal antibodies (Santa-Cruz), respectively.

In vitro interaction analysis and protein kinase assays

Recombinant glutathione-S-transferase (GST) or maltose-binding protein (MBP) fusion proteins of of GRI, GRIp31-96 or the intracellular kinase domains of PRK5 and PRK4 were produced in *E. coli* BL21 cells and purified according to manufacturer's instructions. *In vitro* interaction tests of the extracellular domain of PRK5 with GRI were performed as described (Nakagami *et al.*, 2004). Western analysis for GST-fusion proteins was done using anti-GST antibody (mouse monoclonal antibody; Sigma Aldrich), anti-GRI antibody (rabbit polyclonal antibody raised against the epitope TRKCASGVKCEYGYC, Inbiolabs) or anti-GRI-pep (rabbit polyclonal antibody raised against the epitope VVDQEDDPEYYIL, Inbiolabs), respectively. Radioactive *in vitro* protein kinase assays using myelin-basic protein as an artificial substrate were performed as

described (Idänheimo *et al.*, 2014) in 10 mM HEPES pH 7.4, 1 mM dithriolthetiol with either 10 mM $MgCl_2$ or $MnCl_2$.

Microscopy

PRK5 subcellular localization was analyzed by confocal microscopy on a Leica SP5 II HCS A inverted confocal microscope using a solid state blue laser for CFP, YFP and chloroplast autofluorescence (detection with 465-510 nm, 521-587 nm and 636-674 nm range, respectively).

***In vitro* AtMC9 cleavage assay**

Recombinant His-6 purified AtMC9 protease (Vercammen *et al.*, 2004) and the inactive AtMC9C147AC29A mutant (Belenghi *et al.*, 2007) were pre-activated in assay buffer containing 50 mM MES (pH 5.5), 150 mM NaCl, 10% (w/v) sucrose, 0.1% (w/v) CHAPS and 10 mM DTT for 15 min at room temperature. The proteases were then mixed with the substrate in several pmol quantity ratios and incubated at 30˚C for 30 min. The reaction was terminated by addition of Laemmli SDS-PAGE loading buffer and heating to 95°C for 5 minutes. Proteins were separated on 12% SDS-PAGE gels and transferred to Immobilon P (Millipore) membrane for Western blot analysis. AtMC9 was probed with a rabbit polyclonal antibody (Vercammen *et al.*, 2004) and MBP-tagged substrates with a MBP-tag rabbit polyclonal antibody (Santa-Cruz) and visualised by chemiluminescence (Western Lightning® Plus-ECL, PerkinElmer). In-solution acetyl-2H(3) labeling and subsequent MS/MS analysis of neo N-termini was performed as described (Melzer *et al.*, 2012).

Mass spectrometric analysis

In-solution trideutero-acetyl (<AcD3>)-labeling and subsequent MS/MS analysis of neo N-termini was performed as previously described (Helsens *et al.*, 2008) with minor modifications. Approximately 5 µg of AtMC9 and MBP-$GRI^{25\text{-}168}$ (total amount in the protein mix) were reacted for 90 min at 30˚C in AtMC9 assay buffer supplemented with 2 mM TCEP. The reaction was stopped by raising the pH to 8.0 with NaOH and alkylation of cysteines with 10 mM iodacetamide for 1 h at 30˚C in the dark. The buffer was exchanged to 50 mM triethylammonium bicarbonate buffer. Labeling was performed in solution with a 3-fold molar excess of N-hydroxysuccinimide ester of trideutero-acetate (produced in-house), twice for 1 h at 30˚C. To

quench remaining NHS-ester, a 4-fold molar excess (over NHS-ester) of glycine was added for 10 min at 30˚C. Trypsin digestion was performed overnight, after which the digest was incubated with a 4-fold molar excess of hydroxylamine for 10 min at 30˚C and was subsequently acidified with trifluoroacetic acid (TFA). Peptides were analyzed by LC-MS/MS using a Thermo LTQ Orbitrap XL mass spectrometer. Spectra were identified with the Mascot search algorithm in the TAIR10 database (concatenated with MBP-GRI$^{25-168}$ sequence).

The Mascot search parameters and all identified spectra matching the MBP-GRI$^{25-168}$ sequence were grouped in supporting dataset S01.

In vitro GRIp$^{31-96}$ peptide cleavage by AtMC9 and separation by RP-HPLC

The GRIp$^{31-96}$ peptide was dissolved to a concentration of 1 mM in 5% formic acid and adjusted to pH 3.8 with NaOH. 200 µM GRIp$^{31-96}$ peptide was incubated per 40 µl reaction mixture (pH of the reaction mixtures was adjusted to pH 5.5 with NaOH) containing increasing concentration of recombinant AtMC9 (0, 31, 125 or 500 nM rAtMC9) in AtMC9 assay buffer (supplemented with 40 mM DTT and 40 mM MES buffer). After incubation for 30 min at 30˚C, the reaction was stopped by addition of 5 µl 10% TFA. Cleavage products in the samples were separated by Reverse-Phase High-Performance Liquid Chromatography (RP-HPLC, Agilent Technologies 1200 series) on a 2.1 mm (internal diameter) C18 column in solvent A (2%/98% ACN/$H_2$0, 0.1% TFA) with a gradient increase of 1% solvent B (70%/30% ACN/H_2O, 0.1% TFA) per minute. Buffer controls were run with the same parameters. Peptide elution was monitored by measuring UV absorbance at 280 nm and 1 minute fractions were collected from 24 to 120 min in a 96 well plate. Fractions corresponding to each peak in the 500 nM rAtMC9 sample were measured by MALDI-TOF MS (Ultraflex, Bruker) and the measured masses were linked to GRIp$^{31-96}$ peptide fragments. The fractions of the 0 nM rAtMC9 sample corresponding to the suspected full length GRIp$^{31-96}$ peptide were analyzed by LC-MS/MS using a Thermo LTQ Orbitrap XL mass spectrometer and the correct GRIp$^{31-96}$ mass was deduced from the MS precursor masses. Detected peptides are listed in supporting dataset S01.

Primer sequences

Primers used for cloning are listed in supporting dataset S02.

Sequence analysis

Sequences were aligned using PSI-Coffee (Di Tommaso *et al.*, 2011) at the T-Coffee web server (http://tcoffee.crg.cat/apps/tcoffee/index.html).

Protein structure predictions

Protein structure predictions were done using I-TASSER (Roy *et al.*, 2010) (http://zhanglab.ccmb.med.umich.edu/I-TASSER/) or Phyre^2 (http://www.sbg.bio.ic.ac.uk/phyre2/html/page.cgi?id=index) (Kelley and Sternberg, 2009).

Statistical analysis

Statistical analysis was performed in IBM SPSS Statistics (version 22). Ion leakage and binding data was analyzed using one-way ANOVA using Sidak's post-hoc test. Bacterial growth was analyzed using two-way ANOVA using Tukey's HSD post-hoc test. Plots were created in Sigmaplot and in R.

Acknowledgements

We thank Tuomas Puukko and Leena Grönholm for technical help. We thank Dr. Silke Robatzek and Dr. Sarah K. Coleman for help with radio-ligand binding, Dr. Claudia Jonak for suggestions for analysis of protein kinase activity and Dr. Jan Willem Borst, Prof. Theodorus Galdella, Dr. Silke Robatzek, and Dr. Claudia Jonak for materials. We thank Dr. Mikko Frilander for access to the isotope laboratory at the Institute of Biotechnology, University of Helsinki, and Dr. Jarkko Salojärvi for help with statistics. We thank Drs. Sarah K. Coleman, Pinja Jaspers, Julia Krasensky, Johanna Leppälä, Maija Sierla, and Jorma Vahala for critical comments on the manuscript.

This research was supported by the Academy of Finland Centre of Excellence program and Helsinki University Biocentrum Helsinki program (to JK), Research Foundation-Flanders (grant number G.0038.09N to FVB) and Ghent University (Special Research Fund and Multidisciplinary Research Partnership Biotechnology for a Sustainable Economy to FB), the Swedish Energy agency and Research councils VR, Vinnova and Formas (to HT). AG is supported by a post-doctoral grant from the Academy of Finland (decision #140187); MW is supported by the University of Helsinki (post-doctoral grant and 3-year fund allocation) and the Academy of Finland (decision #275632). JPV was supported by the Finnish Cultural Foundation (grant number 00111000). LT was supported by VIB International PhD Program and EMBO (LTF-776-2013). Financial support for the lab of YH was provided by the Academy of Finland Centre of Excellence programme, the University of Helsinki, the European Research Council Advanced Investigator Grant Symdev, and the Gatsby Foundation.

Author contribution

MW and JPV contributed equally to this work. SS, LT and HHRR contributed equally to this work. MW, JPV, SS, LT, HHRR, HT, KG, FVB, YH and JK designed research and MW, JPV, HH, SS, LT, AG, DK, AL, AS and BB carried out experiments. MW, JPV, and JK wrote the paper. All authors discussed the results and commented on the manuscript.

Conflict of interest

The authors declare no conflict of interest.

References

1. Aker J and de Vries SC (2008) Plasma membrane receptor complexes. *Plant Physiol* 147: 1560-1564.

2. Altenbach D and Robatzek S (2007) Pattern recognition receptors: from the cell surface to intracellular dynamics. *Mol Plant Microbe Interact* 20: 1031-1039.

3. Bauer Z, Gómez-Gómez L, Boller T, and Felix G (2001) Sensitivity of different ecotypes and mutants of *Arabidopsis thaliana* toward the bacterial elicitor flagellin correlates with the presence of receptor-binding sites. *J Biol Chem* 276: 45669-45676.

4. Bayer M, Nawy T, Giglione C, Galli M, Meinnel T, and Lukowitz W (2009) Paternal control of embryonic patterning in *Arabidopsis thaliana*. Science 323: 1485-1488.

5. Belenghi B, Romero-Puertas MC, Vercammen D, Brackenier A, Inzé D, Delledonne M, and Van Breusegem F (2007) Metacaspase activity of *Arabidopsis thaliana* is regulated by S-nitrosylation of a critical cysteine residue. *J Biol Chem* 282: 1352-1358.

6. Blaum BS, Mazzotta S, Nöldeke ER, Halter T, Madlung J, Kemmerling B, and Stehle T (2014) Structure of the pseudokinase domain of BIR2, a regulator of BAK1-mediated immune signaling in *Arabidopsis*. *J Struct Biol* 186: 112-121.

7. Boller T and Felix G (2009) A renaissance of elicitors: perception of microbe-associated molecular patterns and danger signals by pattern-recognition receptors. *Annu Rev Plant Biol* 60: 379-406.

8. Bollhöner B, Zhang B, Stael S, Denancé N, Overmyer K, Goffner D, Van Breusegem F, and Tuominen H (2013) Post mortem function of AtMC9 in xylem vessel elements. New Phytol 200: 498-510.

9. Butenko MA, Vie AK, Brembu T, Aalen RB, and Bones AM (2009) Plant peptides in signalling: looking for new partners. *Trends Plant Sci* 14: 255-263.

10. Castells E and Casacuberta JM (2007) Signalling through kinase-defective domains: the prevalence of atypical receptor-like kinases in plants. *J Exp Bot* 58: 3503-3511.

11. Chang F, Gu Y, Ma H, and Yang Z (2013) AtPRK2 promotes ROP1 activation via RopGEFs in the control of polarized pollen tube growth. *Mol Plant* 6: 1187-1201.

12. Coll NS, Vercammen D, Smidler A, Clover C, Van Breusegem F, Dangl JL, and Epple P (2010) *Arabidopsis* type I metacaspases control cell death. *Science* 330: 1393-1397.

13. Dat JF, Pellinen R, Beeckman T, van de Cotte B, Langebartels C, Kangasjärvi J, Inzé D, and Van Breusegem F (2003) Changes in hydrogen peroxide homeostasis trigger an active cell death process in tobacco. *Plant J* 33: 621-632.

14. Di Tommaso P, Moretti S, Xenarios I, Orobitg M, Montanyola A, Chang JM, Taly JF, and Notredame C (2011) T-Coffee: a web server for the multiple sequence alignment of protein and RNA sequences using structural information and homology extension. *Nucleic Acids Res* 39: W13-W17.

15. Goldman MH, Goldberg RB, and Mariani C (1994) Female sterile tobacco plants are produced by stigma-specific cell ablation. *EMBO J* 13: 2976-2984.

16. Halter T, Imkampe J, Blaum BS, Stehle T, and Kemmerling B (2014a) BIR2 affects complex formation of BAK1 with ligand binding receptors in plant defense. *Plant Signal Behav* doi: http://dx.doi.org/10.4161/psb.28944.

17. Halter T, Imkampe J, Mazzotta S, Wierzba M, Postel S, Bücherl C, Kiefer C, Stahl M, Chinchilla D, Wang X, Nürnberger T, Zipfel C, Clouse S, Borst JW, Boeren S, de Vries SC, Tax F, and Kemmerling B (2014b) The leucine-rich repeat receptor kinase BIR2 is a negative regulator of BAK1 in plant immunity. *Curr Biol* 24: 134-143.

18. He R, Drury GE, Rotari VI, Gordon A, Willer M, Farzaneh T, Woltering EJ, and Gallois P (2008) Metacaspase-8 modulates programmed cell death induced by ultraviolet light and H_2O_2 in *Arabidopsis*. *J Biol Chem* 283: 774-783.

19. Hellens RP, Edwards EA, Leyland NR, Bean S, and Mullineaux PM (2000) pGreen: a versatile and flexible binary Ti vector for *Agrobacterium*-mediated plant transformation. *Plant Mol Biol* 42: 819-832.

20. Helsens K, Timmerman E, Vandekerckhove J, Gevaert K, and Martens L (2008) Peptizer, a tool for assessing false positive peptide identifications and manually validating selected results. *Mol Cell Proteom* 7: 2364-2372.

21. Hoeberichts FA, ten Have A, and Woltering EJ (2003) A tomato metacaspase gene is upregulated during programmed cell death in *Botrytis cinerea*-infected leaves. *Planta* 217: 517-522.

22. Huang WJ, Liu HK, McCormick S, and Tang WH (2014) Tomato pistil factor STIG1 promotes in vivo pollen tube growth by binding to phosphatidylinositol 3-phosphate and the extracellular domain of the pollen receptor kinase LePRK2. *Plant Cell* doi: http://dx.doi.org/10.1105/tpc.114.123281.

23. Idänheimo N, Gauthier A, Salojärvi J, Siligato R, Brosché M, Kollist H, Mähönen AP, Kangasjärvi J, and Wrzaczek M (2014) The *Arabidopsis thaliana* cysteine-rich receptor-like kinases CRK6 and CRK7 protect against apoplastic oxidative stress. *Biochem Biophys Res Commun* 445: 457-462.

24. Jonak C, Beisteiner D, Beyerly J, and Hirt H (2000) Wound-induced expression and activation of WIG, a novel glycogen synthase kinase 3. *Plant Cell* 12: 1467-1475.

25. Kelley LA and Sternberg MJ (2009) Protein structure prediction on the Web: a case study using the Phyre server. *Nat Protoc* 4: 363-371.

26. Kwaaitaal M, Schor M, Hink MA, Visser AJ, and de Vries SC (2011) Fluorescence correlation spectroscopy and fluorescence recovery after photobleaching to study receptor kinase mobility *in planta*. *Methods Mol Biol* 779: 225-242.

27. Lam E and Zhang Y (2012) Regulating the reapers: activating metacaspases for programmed cell death. *Trends Plant Sci* 17: 487-494.

28. Lee H, Chah OK, and Sheen J (2011) Stem-cell-triggered immunity through CLV3p-FLS2 signalling. *Nature* 473: 376-379.

29. Liebrand TW, van den Burg HA, and Joosten MH (2014) Two for all: receptor-associated kinases SOBIR1 and BAK1. *Trends Plant Sci* 19: 123-132.

30. Löcke S, Fricke I, Mucha E, Humpert ML, and Berken A (2010) Interactions in the pollen-specific receptor-like kinases-containing signaling network. *Eur J Cell Biol* 89: 917-923.

31. Melzer IM, Fernández SB, Bösser S, Lohrig K, Lewandrowski U, Wolters D, Kehrloesser S, Brezniceanu ML, Theos AC, Irusta PM, Impens F, Gevaert K, and Zörnig M (2012) The Apaf-1-binding protein Aven is cleaved by Cathepsin D to unleash its anti-apoptotic potential. *Cell Death Differ* 19: 1435-1445.

32. Mittler R, Vanderauwera S, Suzuki N, Miller G, Tognetti VB, Vandepoele K, Gollery M, Shulaev V, and Van Breusegem F (2011) ROS signaling: the new wave? *Trends Plant Sci* 16: 300-309.

33. Murphy E, Smith S, and De Smet I (2012) Small signaling peptides in *Arabidopsis* development: how cells communicate over a short distance. *Plant Cell* 24: 3198-3217.

34. Nakagami H, Kiegerl S, and Hirt H (2004) OMTK1, a novel MAPKKK, channels oxidative stress signaling through direct MAPK interaction. *J Biol Chem* 279: 26959-26966.

35. Pimenta DC and Lebrun I (2007) Cryptides: buried secrets in proteins. *Peptides* 28: 2403-2410.

36. Rawlings ND, Waller M, Barrett AJ, and Bateman A (2014) MEROPS: the database of proteolytic enzymes, their substrates and inhibitors. *Nucleic Acids Res* 42: D503-D509.

37. Roy A, Kucukural A, and Zhang Y (2010) I-TASSER: a unified platform for automated protein structure and function prediction. *Nat Protoc* 5: 725-738.

38. Rozhon W, Mayerhofer J, Petutschnig E, Fujioka S, and Jonak C (2010) ASKΘ, a group-III Arabidopsis GSK3, functions in the brassinosteroid signalling pathway. *Plant J* 62: 215-223.

39. Shiu SH and Bleecker AB (2003) Expansion of the receptor-like kinase/Pelle gene family and receptor-like proteins in Arabidopsis. *Plant Physiol* 132: 530-543.

40. Stone JM and Walker JC (1995) Plant protein kinase families and signal transduction. *Plant Physiol* 108: 451-457.

41. Sundström JF, Vaculova A, Smertenko AP, Savenkov EI, Golovko A, Minina E, Tiwari BS, Rodriguez-Nieto S, Zamyatnin AA, Jr., Välineva T, Saarikettu J, Frilander MJ, Suarez MF, Zavialov A, Ståhl U, Hussey PJ, Silvennoinen O, Sundberg E, Zhivotovsky B, and Bozhkov PV (2009) Tudor staphylococcal nuclease is an evolutionarily conserved component of the programmed cell death degradome. *Nat Cell Biol* 11: 1347-1354.

42. Tang W, Kelley D, Ezcurra I, Cotter R, and McCormick S (2004) LeSTIG1, an extracellular binding partner for the pollen receptor kinases LePRK1 and LePRK2, promotes pollen tube growth *in vitro*. *Plant J* 39: 343-353.

43. Tsiatsiani L, Gevaert K, and Van Breusegem F (2012) Natural substrates of plant proteases: how can protease degradomics extend our knowledge? *Physiol Plant* 145: 28-40.

44. Tsiatsiani L, Timmerman E, De Bock PJ, Vercammen D, Stael S, van de Cotte B, Staes A, Goethals M, Beunens T, Van Damme P, Gevaert K, and Van Breusegem F (2013) The *Arabidopsis* METACASPASE9 degradome. *Plant Cell* 25: 2831-2847.

45. Tsiatsiani L, Van Breusegem F, Gallois P, Zavialov A, Lam E, and Bozhkov PV (2011) Metacaspases. *Cell Death Differ* 18: 1279-1288.

46. Vaddepalli P, Fulton L, Batoux M, Yadav RK, and Schneitz K (2011) Structure-function analysis of STRUBBELIG, an Arabidopsis atypical receptor-like kinase involved in tissue morphogenesis. *PLoS One* 6: e19730.

47. Vahisalu T, Kollist H, Wang YF, Nishimura N, Chan WY, Valerio G, Lamminmäki A, Brosché M, Moldau H, Desikan R, Schroeder JI, and Kangasjärvi J (2008) SLAC1 is required for plant guard cell S-type anion channel function in stomatal signalling. *Nature* 452: 487-491.

48. van der Hoorn RA (2008) Plant proteases: from phenotypes to molecular mechanisms. *Annu Rev Plant Biol* 59: 191-223.

49. Vercammen D, Belenghi B, van de Cotte B, Beunens T, Gavigan JA, De Rycke R, Brackenier A, Inzé D, Harris JL, and Van Breusegem F (2006) Serpin1 of *Arabidopsis thaliana* is a suicide inhibitor for metacaspase 9. *J Mol Biol* 364: 625-636.

50. Vercammen D, Declercq W, Vandenabeele P, and Van Breusegem F (2007) Are metacaspases caspases? *J Cell Biol* 179: 375-380.

51. Vercammen D, van de Cotte B, De Jaeger G, Eeckhout D, Casteels P, Vandepoele K, Vandenberghe I, Van Beeumen J, Inzé D, and van Breusegem F (2004) Type II metacaspases Atmc4 and Atmc9 of *Arabidopsis thaliana* cleave substrates after arginine and lysine. *J Biol Chem* 279: 45329-45336.

683 52. Wang Y, Loake GJ, and Chu C (2013) Cross-talk of nitric oxide and reactive oxygen
684 species in plant programed cell death. *Front Plant Sci* 4: 314.

685 53. Watanabe N and Lam E (2011) Arabidopsis metacaspase 2d is a positive mediator of cell
686 death induced during biotic and abiotic stresses. *Plant J* 66: 969-982.

687 54. Wrzaczek M, Brosché M, and Kangasjärvi J (2013) ROS signaling loops - production,
688 perception, regulation. *Curr Opin Plant Biol* 16: 575-582.

689 55. Wrzaczek M, Brosché M, and Kangasjärvi J (2009a) Scorched earth strategy: Grim
690 Reaper saves the plant. *Plant Signal Behav* 4: 631-633.

691 56. Wrzaczek M, Brosché M, Kollist H, and Kangasjärvi J (2009b) *Arabidopsis* GRI is
692 involved in the regulation of cell death induced by extracellular ROS. *Proc Natl Acad Sci*
693 *USA* 106: 5412-5417.

694 57. Wrzaczek M, Brosché M, Salojärvi J, Kangasjärvi S, Idänheimo N, Mersmann S,
695 Robatzek S, Karpinski S, Karpinska B, and Kangasjärvi J (2010) Transcriptional
696 regulation of the CRK/DUF26 group of receptor-like protein kinases by ozone and plant
697 hormones in Arabidopsis. *BMC Plant Biol* 10: 95.

698 58. Zhang CJ, Zhao BC, Ge WN, Zhang YF, Song Y, Sun DY, and Guo Y (2011) An
699 apoplastic h-type thioredoxin is involved in the stress response through regulation of the
700 apoplastic reactive oxygen species in rice. *Plant Physiol* 157: 1884-1899.

Figure legends

Figure 1: The LRR RLK PRK5 is required for GRI-peptide-induced ion leakage.

A Infiltration of $GRIp^{65-84}$ induced cell death similar to $GRIp^{31-96}$. Bacterially produced 37 nM GST, GST-$GRIp^{31-96}$ or biochemically pure GRI-peptides ($GRIp^{31-96}$, $GRIp^{31-51}$, $GRIp^{47-68}$, $GRIp^{65-84}$, $GRIp^{80-96}$) were infiltrated into leaves of Col-0 plants.

B Infiltration of increasing concentrations of $GRIp^{65-84}$ into Col-0 leaves, electrolyte leakage was measured after 12 hours. Background (red line) shows ion leakage from infiltration of leaves with increasing concentrations of (inactive) $GRIp^{80-96}$.

C Infiltration of leaves with 37 nM $GRIp^{31-96}$ induced elevated ion leakage in Col-0 and *prk4*, but not in *prk5-1* or *prk5-2*. Infiltration with GST caused the same background effect for all lines.

D Genomic complementation of *prk5* rescues the insensitivity to induction of elevated ion leakage by $GRIp^{31-96}$.

E Enzymatic superoxide production from xanthine/xanthine oxidase (XXO) induced more electrolyte leakage in *gri* compared to Col-0 or *prk5-1*, *prk5-2* and *prk4* after infiltration into leaves. Infiltration with xanthine buffer (X) was used as control.

Data information All panels show average ± standard deviation (SD) of four replicates consisting of four leaf disks each. Asterisks indicate statistically significant differences from GST infiltration (panels A, C, D), from infiltration with (inactive) $GRIp^{80-96}$ (panel B) or from Col-0 (panel E) according to Sidak's test ($P<0.05$). All experiments were repeated at least four times with similar results.

Figure 2: PRK5 is an atypical, enzymatically inactive, RLK.

A PRK5 domain structure: SP signal peptide (aa 1-39), LRR leucine-rich repeat, RPT internal repeat, LC region of low complexity, TM transmembrane domain (aa 282-304), EM Y-based sorting/endocytosis motif (YSSM; aa 670-673).

B PRK5-CFP localized to the cell periphery in Col-0 mesophyll protoplasts.

C-F Co-localization of PRK5-CFP and PM localized CAAX-YFP in Col-0 mesophyll protoplasts. **C** overlay **D** PRK5-CFP (465-510 nm) **E** CAAX-YFP (521-587 nm) **F** chloroplast (636 – 711 nm).

G Alignment of subdomains VIb and VII of the catalytic core of the kinase domains of active (BRI1, FLS2, EFR, CRK7) and inactive RLKs (PRK4, PRK5, BIR2, SUB). Residues marked in green highlight conservation of the consensus of active protein kinases while residues highlighted in red indicate deviations from the consensus sequence. An alignment of the full kinase domains for the RLKs used in this figure can be found in Fig. S11A.

H Kinase activity of PRK5 in *in vitro* phosphorylation assays using γ^{32}P-ATP and MYELIN BASIC PROTEIN (MBP) as a substrate in the presence of 10 mM $MnCl_2$. GST- PRK5 and GST- PRK4 did not show kinase activity. Mutation of conserved residues in kinase subdomains VIb and VII to reconstitute the consensus kinase domain motif restored GST- PRK5^{H500DA520G} kinase activity. GST-CRK7 was used as positive control. Upper panel shows autoradiograph, lower panel shows the Coomassie-stained 15% SDS-polyacrylamide gel.

Data information Experiments in **B-F** were repeated three times with similar results.

Figure 3: **A 20-aa peptide binds to the extracellular domain of PRK5.**

A *In vitro* produced ^{35}S-labeled ectodomains of PRK5 (PRK5$^{40-281}$) or PRK4 (PRK4$^{40-279}$) were incubated with bacterially produced GST, GST-GRI or GST-GRI$^{31-96}$ and purified. GST-GRI$^{31-96}$ but not GST directly bound to the ectodomain of PRK5. Binding of GST-GRI to PRK5 ectodomain and binding of GST-GRI$^{31-96}$ and GST-GRI to the ectodomain of PRK4 was strongly reduced. Upper part: autoradiograph, lower part: Coomassie-stained 12% SDS-polyacrylamide gel. Asterisks in the Coomassie-stained gel indicate GST, GST-GRI and GST-GRI$^{31-96}$, respectively. Fig. S12 shows Western blot of the GST-tagged proteins.

B Infiltration of 37 nM GST, GRIp$^{31-96}$, GRIp$^{65-84}$ or Y-GRIp$^{65-84}$ into Col-0 or *prk5-2* leaves. Tyrosine-labeled GRIp$^{65-84}$ still induced cell death in Col-0 but not in *prk5-2* plants.

C ^{125}I-labeled Y-GRIp$^{65-84}$ (0.46 nM) bound specifically to Col-0 membrane fractions (light grey bars), the binding was significantly reduced in *prk5* plants. Excess of non-radioactive Y-GRIp$^{65-84}$ (10 µM) reduced binding to background levels (dark grey bars; all bars show average of two samples, triangles show individual data points).

D Immunoprecipitation of PRK5-c-myc, PRK4-c-myc or YFP expressed in protoplasts with rabbit polyclonal anti-c-myc antibody, blotted with mouse monoclonal anti-c-myc antibody.

E Binding of ^{125}I-Y-GRIp$^{65-84}$ (0.46 nM) to immunoprecipitates (using anti-c-myc antibodies) from *prk5-2* protoplasts transfected with PRK5-c-myc, PRK4-c-myc or YFP, respectively.

Binding was competed out with 10 µM unlabeled Y-GRIp$^{65-84}$. Bars show average of two samples, triangles show individual data points. Western blot is shown in panel **D**.

F Analysis of ^{125}I-Y-GRIp$^{65-84}$ (0.46 nM) binding competed out with increasing amounts of unlabeled Y-GRIp$^{65-84}$ to Col-0 membrane extracts. 50% inhibition (IC_{50}) occurred at 25.2 nM. Red line shows binding average competition according to a sigmoid curve, dotted lines show 95% confidence intervals, circles show data points.

G Excess of GRIp$^{65-84}$ (10 µM) but not of GRIp$^{31-96}$ or other peptides (GRIp$^{31-51}$, GRIp$^{47-68}$, GRIp$^{80-96}$) competed the binding of 0.46 nM ^{125}I- Y-GRIp$^{65-84}$ to membrane extracts from Col-0 (all bars show average of two samples, triangles show individual data points).

Data information Panels **B** shows average ± standard deviation (SD) of four replicates consisting of four leaf disks each. Asterisks in **B** mark statistically significant differences from infiltration with GST according to Sidak's test (P<0.05). All experiments were repeated three times with similar results.

Figure 4: Processing of GRI-peptide by METACASPASE9 is required for induction of elevated ion leakage.

A Recombinant AtMC9 (rAtMC9) cleaved GRI$^{25-168}$ *in vitro*. Bacterially produced MBP-GRI$^{25-168}$ (from 0 to 2 pmol left to right) was incubated with 1 pmol rAtMC9 or inactive rAtMC9^{mut} (rAtMC9C^{147}AC^{29}A) and cleavage products were analysed by Western blot with anti-MBP and anti-AtMC9 antibodies. Numbered arrowheads (from top to bottom, with molecular weights) indicate: 1: MBP-GRI$^{25-168}$, 2: MBP^{MCS}, 3: rAtMC9-cleaved MBP-GRI$^{25-168}$, 4: N-terminal domain + p20 + p10 subunits of AtMC9, 5: p20 + p10 subunits of AtMC9, 6: N-terminal domain + p20 subunit of AtMC9, 7: p20 subunit of AtMC9.

B Infiltration of wild type, *prk5-1* and *atmc9-1* leaves with37 nM GRIp$^{31-96}$, GRIp$^{65-84}$, GRIp$^{68-78}$ or GST. GRIp$^{65-84}$ and GRIp$^{68-78}$ but not GRIp$^{31-96}$ were able to induce elevated ion leakage in the *atmc9-1* mutant.

C Schematic representation of the GRI and the cleavage sites for rAtMC9. The cleavage product detected in Western analysis with anti-MBP antibody is shown as black bar. Mass spectrometric analysis of MBP-GRI$^{25-168}$ cleavage with rAtMC9 provided evidence for cleavage after SKTR and KANK; further analysis of GRIp$^{31-96}$ cleavage by rAtMC9 provided evidence for cleavage

after SK, SKTR and after KKIKK. The position of the resulting 11-aa long peptide (^{68}LLVSHYKKIKK^{78}) is indicated by a white inset.
D Infiltration of Col-0 leaves with 37 nM of GRIp$^{65-84}$, GRIp$^{68-78}$, Y-GRIp$^{68-78}$, GRIp$^{31-96}$, or GST. Y-GRIp$^{68-78}$ showed similar activity in cell death induction compared to the other GRI-derived peptides.
E ^{125}I-labeled Y-GRIp$^{68-78}$ (0.46 nM) bound specifically to Col-0 membrane fractions (light grey bars), the binding was significantly reduced in *prk5-1* and *prk5-2* plants. Excess of non-radioactive Y-GRIp$^{65-84}$ (10 µM) reduced binding to background levels (dark grey bars; all bars show average of four samples, triangles show individual data points).
F Excess of GRIp$^{68-78}$ and GRIp$^{65-84}$ (10 µM) but not of GRIp$^{31-96}$ or other peptides (GRIp$^{31-51}$, GRIp$^{47-68}$, GRIp$^{80-96}$) competed the binding of 0.46 nM ^{125}I- Y-GRIp$^{68-78}$ to membrane extracts from Col-0 (all bars show average of four samples, triangles show individual data points).
G Saturation binding curve for ^{125}I-Y-GRIp$^{68-78}$ to Col-0 membrane extracts. Specific binding was calculated by subtracting non-specific binding from the total binding. The affinity of ^{125}I-Y-GRIp$^{68-78}$ to the receptor (Kd=1.9 nM) was calculated by non-linear regression analysis. Scatchard plot is shown in Fig. SI7.
Data information Panels **B** and **D** show average ± standard deviation (SD) of four replicates consisting of four leaf disks each. Asterisks in **B** and **D** mark statistically significant differences from infiltration with GST according to Sidak's test (P<0.05). Asterisks in **E** and **F** mark statistically significant differences from peptide binding to Col-0 membrane fractions without competitor according to Sidak's test (P<0.01). All experiments were repeated three times with similar results.

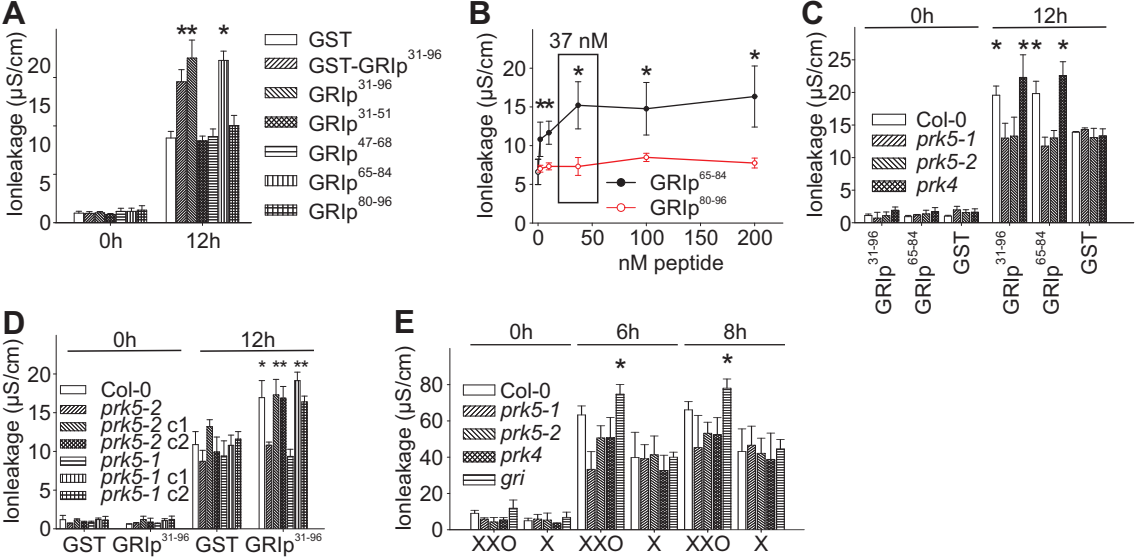
A
Ionleakage (µS/cm)
0h
12h
GST
GST-GRIp31-96
GRIp31-96
GRIp31-51
GRIp47-68
GRIp65-84
GRIp80-96
B
37 nM
Ionleakage (µS/cm)
GRIp65-84
GRIp80-96
nM peptide
C
0h
12h
Ionleakage (µS/cm)
Col-0
prk5-1
prk5-2
prk4
GRIp31-96
GRIp65-84
GST
D
0h
12h
Ionleakage (µS/cm)
Col-0
prk5-2
prk5-2 c1
prk5-2 c2
prk5-1
prk5-1 c1
prk5-1 c2
GST GRIp31-96 GST GRIp31-96
E
0h
6h
8h
Ionleakage (µS/cm)
Col-0
prk5-1
prk5-2
prk4
gri
XXO X XXO X XXO X

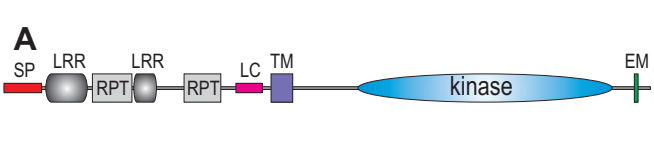

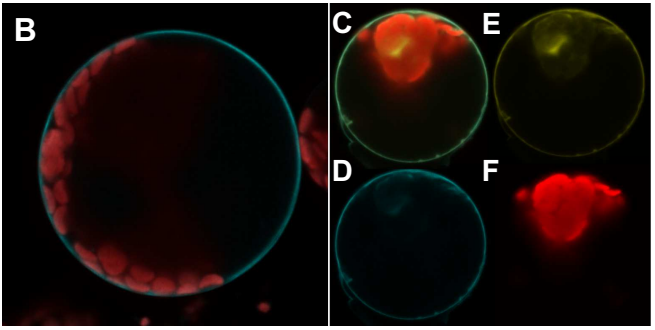

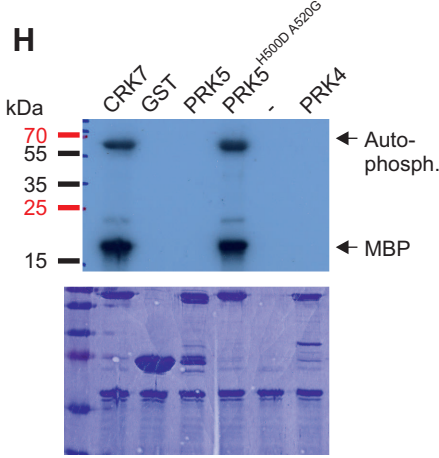

G

```
                                    VIb                                VII
PRK5          115 ELPTLTIPHGHMKSSNIVLDDSFEPLLTDYALRPMMS--- 149
PRK4          118 ELTTLTIPHGHLKSSNVVLDESFEPLLTDYALRPVMN--- 152
BIR2          108 GCR-PPILHQNICSSVILIDEDFDARIIDSGLARLMV--- 143
BRI1          118 NCS-PHIIHRDMKSSNVLLDENLEARVSDFGMARLMS--- 153
FLS2          119 GYG-FPIVHCDLKPANILLDSDRVAHVSDFGTARILG--F 155
EFR           129 HCH-DPVAHCDIKPSNILLDDDLTAHVSDFGLAQLLYKYD 167
CRK7          117 DSR-LTIIHRDLKASNILLDADMNPKIADFGMARIFG--- 150
SUB           120 VCQ-PPVVHQNFKSSKVLLDGKLSVRVADSGLAYMLP--- 153
                      : * .: .: :::* .    : * .    ::
Consensus kinase domain     HRDLK  N           DFG
```

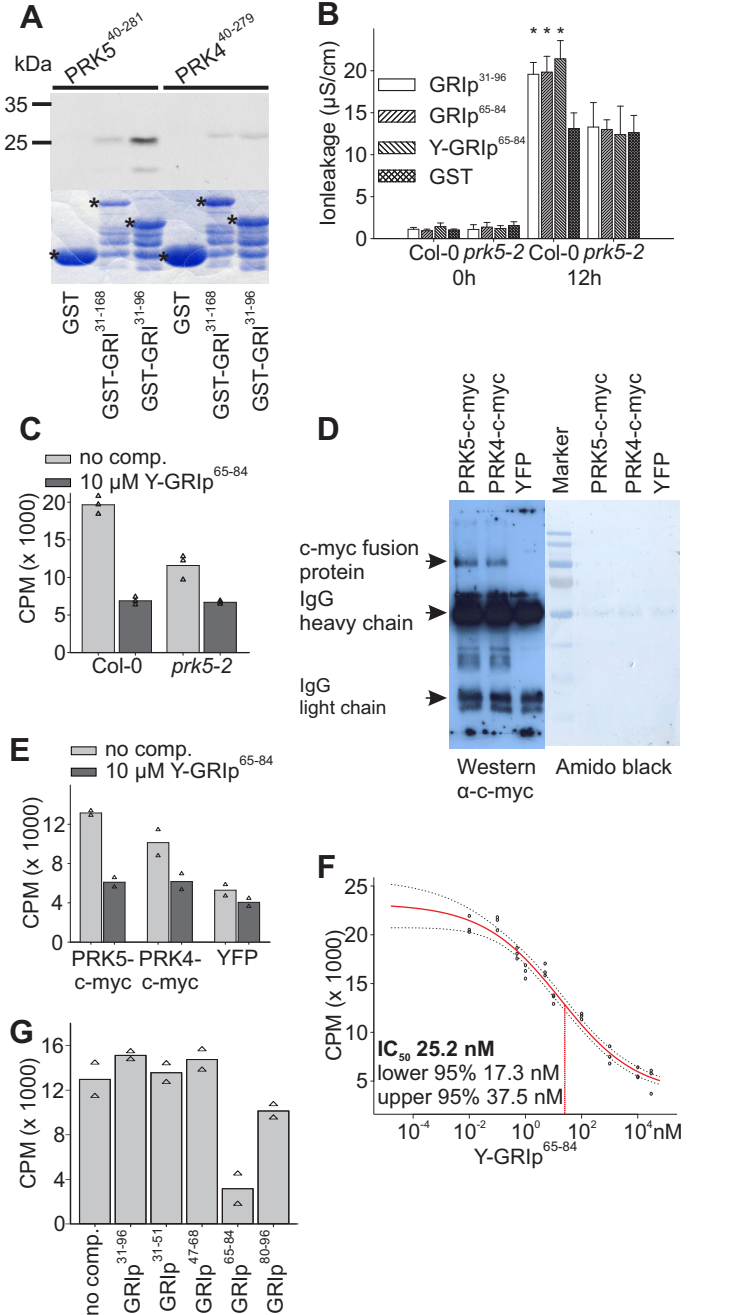
A
kDa
PRK5 40-281
PRK4 40-279
35
25
GST
GST-GRI 31-168
GST-GRI 31-96
GST
GST-GRI 31-168
GST-GRI 31-96
B
Ionleakage (µS/cm)
GRIp 31-96
GRIp 65-84
Y-GRIp 65-84
GST
Col-0 prk5-2 Col-0 prk5-2
0h
12h
C
no comp.
10 µM Y-GRIp 65-84
CPM (x 1000)
Col-0
prk5-2
D
PRK5-c-myc
PRK4-c-myc
YFP
Marker
PRK5-c-myc
PRK4-c-myc
YFP
c-myc fusion protein
IgG heavy chain
IgG light chain
Western α-c-myc
Amido black
E
no comp.
10 µM Y-GRIp 65-84
CPM (x 1000)
PRK5-c-myc
PRK4-c-myc
YFP
F
CPM (x 1000)
IC50 25.2 nM
lower 95% 17.3 nM
upper 95% 37.5 nM
Y-GRIp 65-84
nM
G
CPM (x 1000)
no comp.
GRIp 31-96
GRIp 31-51
GRIp 47-68
GRIp 65-84
GRIp 80-96

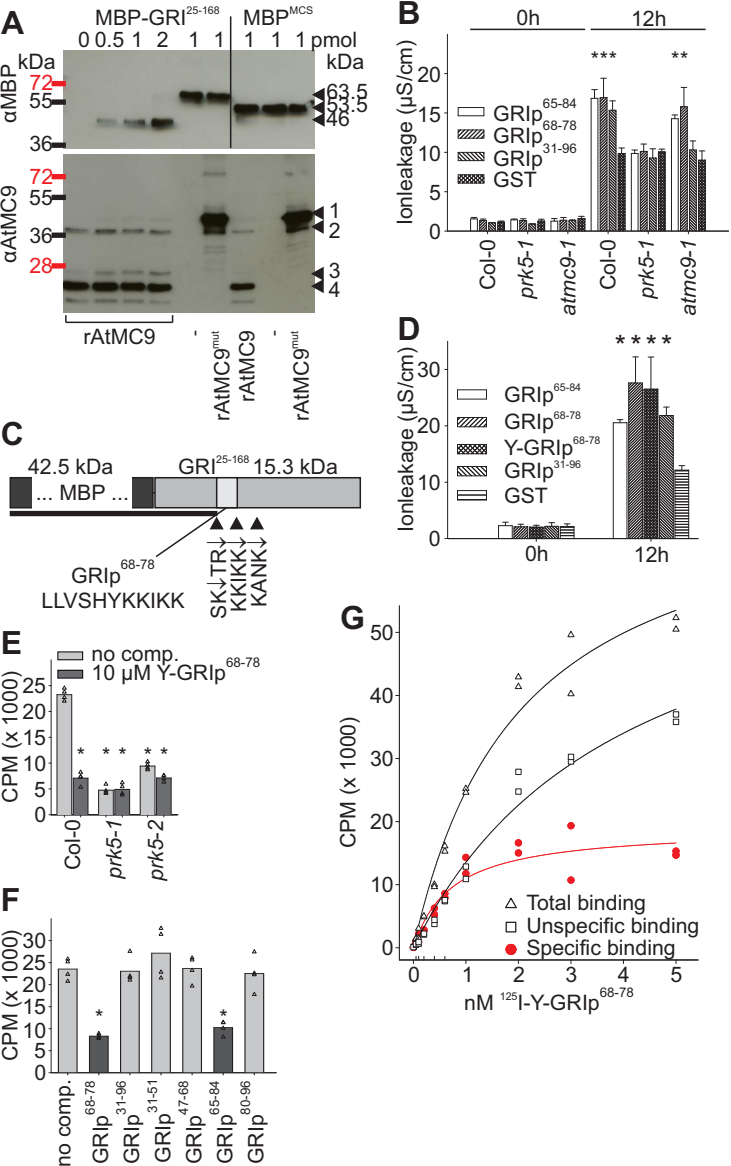
A
MBP-GRI25-168
MBPMCS
0 0.5 1 2 1 1 1 1 1 pmol
kDa
αMBP
72
55
36
63.5
53.5
46
αAtMC9
72
55
36
28
1
2
3
4
rAtMC9
-
rAtMC9mut
rAtMC9
-
rAtMC9mut
B
0h
12h
Ionleakage (µS/cm)
GRIp65-84
GRIp68-78
GRIp31-96
GST
***
**
Col-0
prk5-1
atmc9-1
C
42.5 kDa
... MBP ...
GRI25-168 15.3 kDa
GRIp68-78
LLVSHYKKIKK
SK↓TR↓
KKIKK↓
KANK↓
D
Ionleakage (µS/cm)
GRIp65-84
GRIp68-78
Y-GRIp68-78
GRIp31-96
GST
****
0h
12h
E
no comp.
10 µM Y-GRIp68-78
CPM (x 1000)
Col-0
prk5-1
prk5-2
F
CPM (x 1000)
no comp.
GRIp68-78
GRIp31-96
GRIp31-51
GRIp47-68
GRIp65-84
GRIp80-96
G
CPM (x 1000)
Total binding
Unspecific binding
Specific binding
nM 125I-Y-GRIp68-78